

NUMERICAL SIMULATION OF RIVETING PROCESS USING BLIND RIVET

L. Witek

*Rzeszow University of Technology, Department of Mechanical Engineering and Aeronautics;
35-959 Rzeszow, 8 Powstancow Warszawy Ave.; Poland. E-mail: lwitek@prz.rzeszow.pl
Received 13 07 2005, accepted 09 06 2006*



Lucjan WITEK, Ph.D. Eng.

Was born in 1972. Graduated in 1997 with M.Sc. degree in mechanical engineering (specialization: aerospace), Ph.D. degree in 2002 (discipline: mechanics), both from the Rzeszow University of Technology, Poland. Currently assistant professor at Department of Mechanical Engineering and Aeronautics of Rzeszow University of Technology. Research focuses on fatigue and fracture studies, non-linear stress analysis of mechanical and aircraft structures, and analysis of stability of thin-walled structures. Since 1997 has worked as a university lecturer in the field of strength of aircraft structures and turbo machinery, strength of material and finite element method. In 2003 given NATO Fellowship Organization award. Participant of NATO Postdoctoral Fellowship at Institute for Aerospace Research, National Research Council-Canada, Ottawa.

Abstract. This paper is concerned with an analysis of the mechanical phenomena occurring in the process of blind riveting. Blind rivets are commonly used in the aviation industry and allow riveting with one-sided access. To solve this problem, the finite element method was used. In results of the nonlinear computation performed for a joint containing one rivet, the stress distribution in the separate phases of riveting were analyzed. The plots of riveting force in function of rivet core displacement for different friction coefficients between the rivet and the core and the plastic strain distribution also were obtained. The main purpose of this work was to obtain the initial stress distribution occurring in the rivet and sheets after the mandrel was broken. This analysis showed that after finishing the riveting process the initial stresses occurring in the rivet have high values.

Keywords: blind rivet, aircraft technology, stress analysis, FEM, initial stresses.

Introduction

Riveted joints still play a major role in assembling aircraft structures. The main advantage of this type of joints is basically the repeatability of strength and fatigue properties. Riveted joints also have certain disadvantages, e.g. large labor consumption, but they are still widely used in the aviation industry. In the manufacturing process of many airframe components such as wings, flaps, ailerons or tail units, special blind rivets, which enable closed section of structure to be riveted, must be used. The technological process of blind riveting is not very complicated. Moreover, because of the low cost of blind rivets nowadays, these rivets are commonly used not only in aviation but also in other branches of industry.

For many years, several studies concerned with the increase in the strength of riveted joints have been performed. In the past, these investigations were mainly based on experimental tests because the analytical description of phenomena occurring in riveting or shear process is very complex. Results of several of the latest investigations devoted to the problem of maximum load, stress distribution, or fatigue life of riveted joints were

described by Fitzgerald and Cohen, DiBattista and Adamson, Lucas, Witek, Terada, Galatolo and Nillson, Urban, and Kelly [4, 3, 15, 22, 18, 6, 19, 8].

Rapid development of many numerical techniques in connection with contemporary multiprocessor supercomputers with huge computational power led to the possibility of many nonlinear engineering problems such as contact and plasticity being solved numerically. In the study by Fung and Smart, the authors estimated the initial stress and strain occurring in a riveted lap joint [5]. In this paper, the influence of friction and thickness of connected sheets on the preliminary stress distribution is also examined. The problem of numerical evaluation of the limiting load capacity of sheared riveted joints is also described by Langrand et al. [10–12]. Deng and Hutchinson described the numerical investigation of a phenomenon occurring in the riveting process using a classical solid rivet [2]. Using nonlinear FE analysis, the authors specified the separate phases of riveting concerned with variability of riveting force. An interesting study is the work by Al-Emrani and Kliger in which a riveted bracket of a railway bridge was investigated [9]. In this work, the authors considered the

detailed FE model of joint consisting of 10 rivets.

A similar problem of numerical analysis of riveted joints was also described by Xiong, Witek, Liao et al., Neves et al., Liu and Sawa, and Karaoglu and Kuralay [24, 22, 20, 23, 21, 13, 17, 14, 7].

In this study, attention is focused on the mechanical phenomena occurring in the process of blind riveting. The main purpose is to estimate the initial stress distribution occurring in the riveted joint after breaking of the mandrel. This paper is a continuation of work [21] in which the mandrel of a rivet was assumed to be a rigid spherical surface. In this study, the mandrel of the rivet is defined as 3-dimensional body made of the elastic-plastic material.

1. Analysis of initial stress forming in the process of blind riveting

The subject of investigation is a separated fragment of single-riveted lap joint, consisting of one blind rivet (diameter 3.2 mm) and two sheets (upper and lower) with thicknesses of 1 mm and widths of 20 mm. Due to the complexity of the problem (nonlinear material, contact and nonlinear analysis) the investigation was limited to a joint consisting of one rivet only. Additionally, the presence of the symmetrical plane (X-Y plane) enabled only half of the model to be analyzed. Two can therefore multiply the resulting riveting forces on the plots, obtained in this work.

To create a model of the joint and define the loads and boundary conditions, the program MSC-Patran 2004 was used [16].

Figure 1 shows the numerical model with components of the joint distinguished before riveting. In this figure, five pairs of surfaces which can potentially be in contact during the riveting process are additionally shown. In pairs 1-3, the contact with small sliding is assumed [1]. The contact with small sliding can be used for modeling contact phenomena unless displacement of one surface along the second is smaller than the size of the finite element used. In the 4th and 5th pair, contact with large sliding is additionally defined. The friction coefficient between contact surfaces is set as 0.1. In certain computations, friction coefficients of 0.05 and 0,15 were also assumed.

The finite element model, shown in figure 2 consists of 5860 solid, HEX-8 elements. Two characteristic control points, presented in this figure, were defined to control the stresses in the rivet during the successive increase in riveting force. In FE simulation, the top part of the rivet and tips of the sheets were fixed while the displacement vector of 2 mm was applied to the end of the core.

The material of the lower and upper sheets was defined as linear-elastic with Young's modulus 72000 MPa and Poisson's ratio 0.3 (for aluminum alloy PA-7). A discrete characteristic of the elastic-plastic rivet material with isotropic hardening, presented in figure 3b on the basis of the real stress-plastic strain characteristic (Fig 3a). For alloy PA-20, was defined (taken from Polish standard PN-79/H82160). The mandrel is made of low

tensile steel with Young modulus 210000 MPa and yield point of 350 MPa.

3. Results of FE simulation

The ABAQUS v. 6.4.5 program was used for stress analysis of the riveted joint [1]. All computations were performed on a 2-processor Sun Ultra Enterprise 3000 workstation in the Computer Centre of the Rzeszow University of Technology. In numerical calculation, the nonlinear Newton-Raphson procedure and a theory of large displacement, implemented into the ABAQUS v.6.4 solver were used [16]. In the Newton-Raphson method, a displacement vector of 2 mm) on the small portion of the load was first divided (Fig 2). In consecutive steps of the nonlinear analysis, these parts of the load were added to the load from the previous step. Circles on the plots presented in figure 6, 7 and 9 marks the values of the riveting forces for successive steps of analysis. For all results, Megapascal (MPa) units were used to describe the fields of stress.

Figures 4 and 5 show respectively the plastic strain and Von Mises stress distribution for the joint in the early and final phase of riveting.

As can be seen in figure 4, in the first stage of riveting, the plastic strain area in the vicinity of the bottom part of rivet is located. In this phase, the spherical mandrel head comes into contact with the rivet and rapid growth of the riveting force shown in figure 6 is observed. The maximum value of stress in the core (309 MPa) occurs in the top part, where the necking is located. In this stage of loading, plastic strains in the mandrel are not observed (Fig 4a).

Before finishing the riveting process, the stresses in the rivet achieve 329 MPa (while in the core - 402 MPa (Fig 5b). On the top part of core, the plastic strain value of 0.25 is observed in this advanced state of plastic deformation (Fig 5a).

Figure 6 presents the plots of riveting forces as a function of the rivet core displacement for the elastic-plastic and linear-elastic material of the mandrel. The first curve (defined for the elastic-plastic material of mandrel) can be divided into three characteristic segments with different slope (three phases of riveting). In the first stage, the spherical tip of the mandrel comes into contact with the rivet and rapid growth in the riveting force is observed. The bottom part of the rivet then expands and a formed rivet head is created (second phase, where the force is slowly increased). In the finish stage of riveting, the advanced plastic deformation is observed in the mandrel (Fig 5a). In this phase, the plot of the riveting force is almost flat. 2 must multiply the value of force to breakage of core obtained in this analysis (480 N) because in computation only half of the ax symmetric model was considered (Fig 6). Thus, the maximum value of the riveting force for a blind rivet with diameter 3.2 mm was estimated as 960 N. The maximum value of the riveting force is observed for the mandrel top displacement of 1.8 mm. For a displacement of more than 1.8 mm, the core is broken and the riveting process is finished.

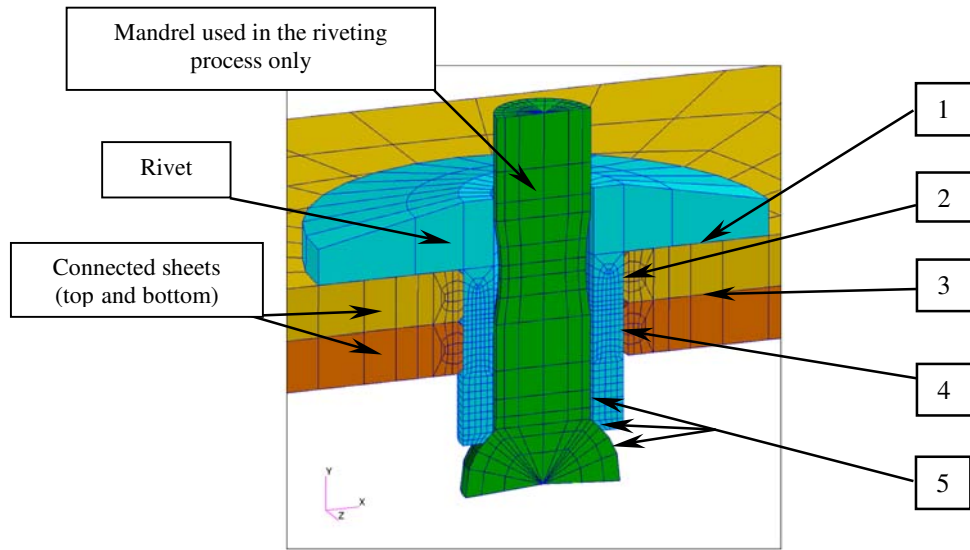


Fig 1. Model of joint components before riveting with the contact surfaces defined

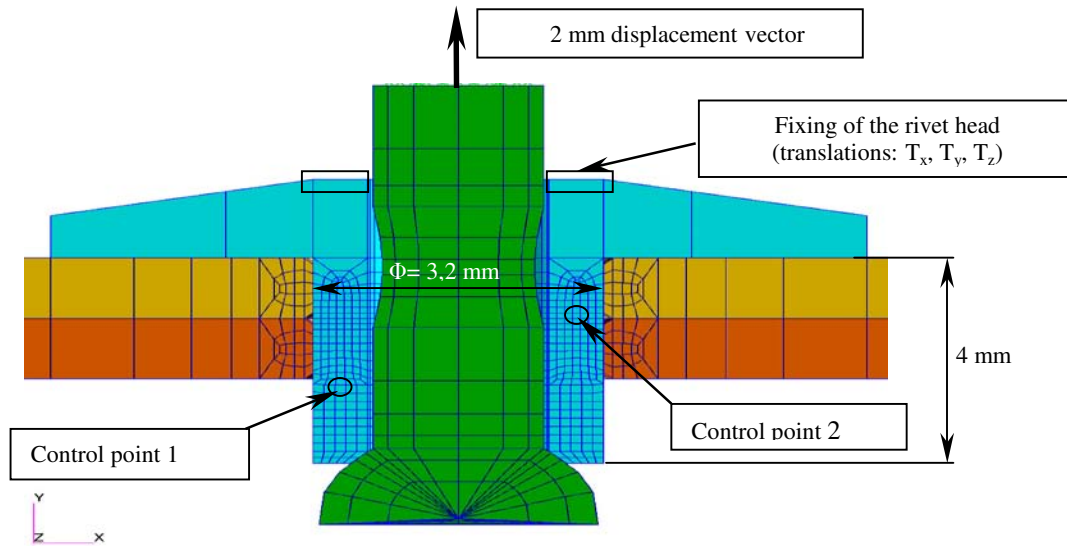


Fig 2. Model of the joint with defined load and boundary conditions for the riveting process

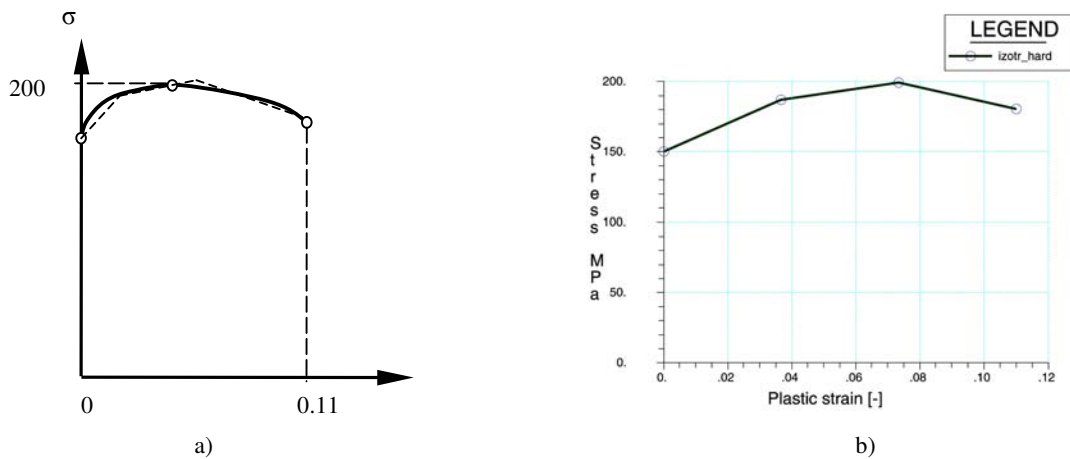


Fig 3. A plot of stress vs. plastic strain for the alloy PA-20 (a) and the discrete characteristic of this material used in computation (b)

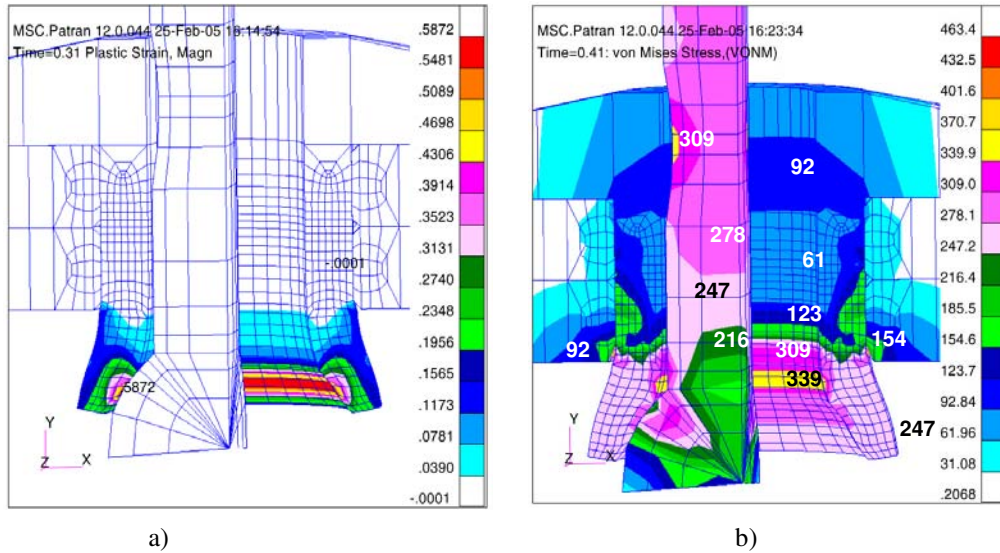


Fig 4. The plastic strain (a) and Von Mises stress (b) distribution in the early stage have riveting (for displacement of core: 0.6 mm)

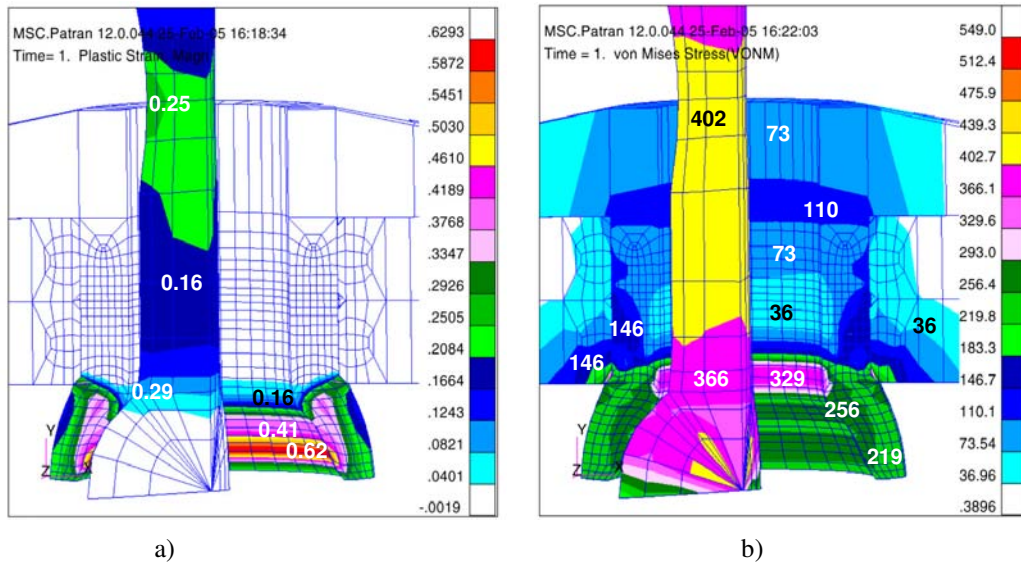


Fig 5. The plastic strain (a) and Von Mises stress (b) distribution in the final phase of riveting (displacement of core – 2 mm)

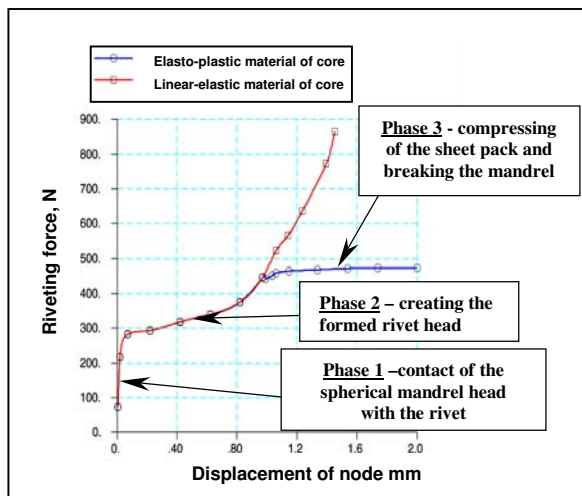


Fig 6. Plot of riveting forces in function of the rivet mandrel displacement for elastic-plastic material of mandrel (circular marks) and linear-elastic material of mandrel (square marks)

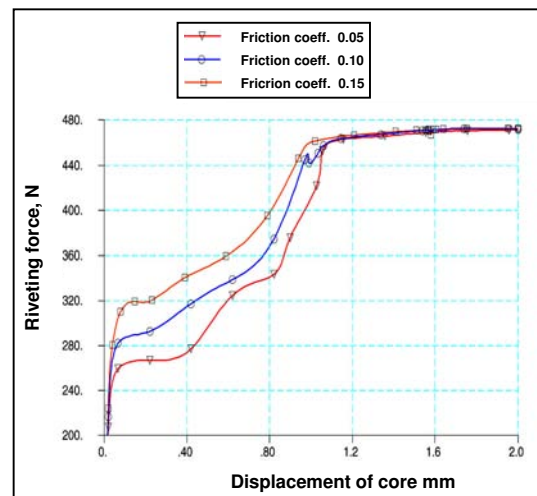


Fig 7. Plot of riveting forces for different friction coefficients defined between the rivet and the spherical surface of mandrel

In this work, the influence of the friction coefficient on the shape of riveting characteristics, presented in figure 7 was also analyzed. As seen from this figure, for a curve with friction 0.05 (i.e. for a rivet first lubricated), the process of formed rivet head creation is beginning by lower force, but the maximum riveting force is the same for all curves considered.

The last phase of riveting begins when the successive rapid growth of the force in the mandrel occurs. In this stage, the pack of sheets is compressed. After that, the rivet mandrel is broken but residual stresses in the joint remain. These stresses are also called initial or preliminary.

The initial stress distribution (after broken of the mandrel) in riveted joints is presented in figure 8. The zone of the maximum residual Von Mises stress (164 – 281 [MPa]) is located at the bottom part of the rivet, where the formed rivet head was created. In the shearing section of the rivet, the stress ranges between 30 and 70 [MPa] (Fig 8b). Residual stress around the holes of sheets reaches 129 MPa for the bottom sheet and 46 MPa for the top sheet (Fig 8a).

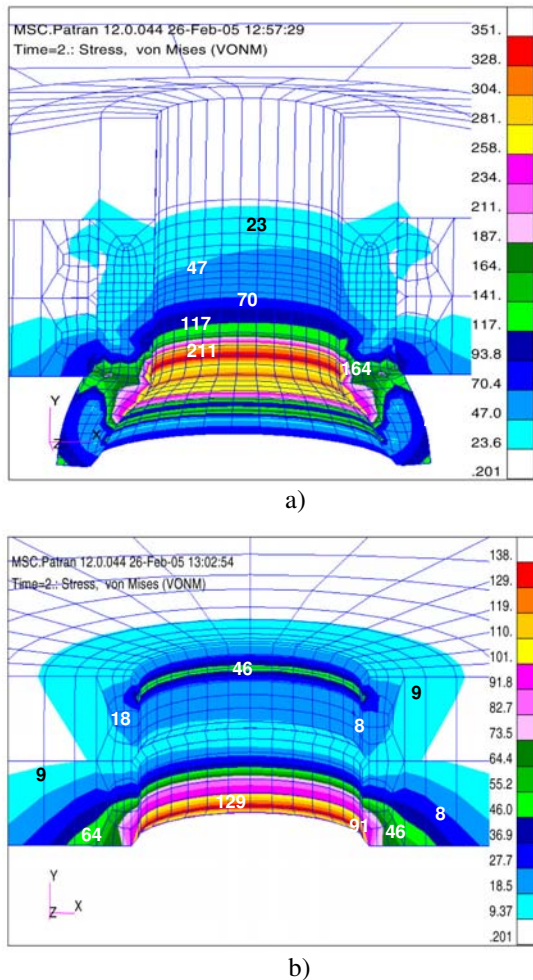


Fig 8. Residual Von Mises stress distribution for sheets (a) and for rivet (b) after riveting process

The values of current stresses under the riveting process and the values of initial stresses for control points No 1 and 2 (Fig 2) are shown in figure 9. As seen from

this figure, in the shearing section of the rivet (point No 2), the Von Mises stress is about 35 MPa, while the tensile stress (Y-component) is about 10 MPa. These stresses can have an influence on the limiting load capacity of a joint.

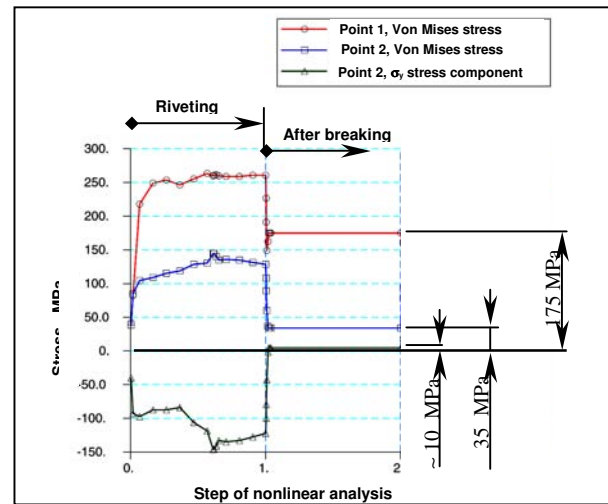


Fig 9. Values of stresses for control points No 1 and 2 during the riveting process

Conclusions

This paper presents the results of complex, static calculation of a blind riveted lap joint. To solve the problem, multi-step numerical FE analysis was carried out. In the results of the nonlinear calculation, stress and strains distributions and the plots of riveting forces in function of the mandrel displacement were generated. The influence of the friction coefficient on the final shape of the riveting characteristic was also obtained. The main result of this work is the initial stress distribution for a blind riveted lap joint.

The following remarks can be formulated based on the numerical results carried out through the work:

1. The residual stresses in the shearing section of the rivet have considerable values and can have a negative influence on the limiting load capacity of a joint.
2. The influence of the friction coefficient between the rivet and the mandrel head is negligible from the point of view of the value of the final riveting force or the shape of the formed rivet head.
3. Residual stress around the holes of sheets achieves a high value. The additional stress concentration concerned with tension in this zone with embedded circular pass can cause a decrease in both static and fatigue strength of a joint.

Acknowledgements

Special thanks for Prof Dr Habil Henryk Kopecki from Rzeszow University of Technology for his support and scientific care during the preparation of the author's doctoral thesis.

References

1. ABAQUS User's Manual, Ver. 6.4. – Abaqus Inc., 2004.
2. **Deng X., Hutchinson J. W.** The clamping stress in a cold-driven rivet // *Int. J. Mech. Sci.* – 1998. – Vol. 40, No 7. – P. 683–694.
3. **DiBattista J., Adamson D., Kulak G.** Fatigue strength of riveted connections // *Journal of Structural Engineering.* – 1998. – Vol 24, No 7. – P. 792–797.
4. **Fitzgerald T.J., Cohen J. B.** Residual stresses in and around rivets in clad aluminum alloy plates // *Material Science and Engineering.* – 1994. – An. 188. – P. 51–58.
5. **Fung C-P., Smart J.** Riveted single lap joints. Part 1: numerical parametric study // *Proc. Inst. Mech. Eng.* – 1997. – Vol 211, part G. – P. 13–27.
6. **Galatolo R., Nilsson K.-F.** An experimental and numerical analysis of residual strength of butt-joints panels with multiple site damage // *Engineering Fracture Mechanics.* – 2001. – Vol 68. – P. 1437–1461.
7. **Karaoglu C., Kuralay N. S.** Stress analysis of a truck chassis with riveted joints // *Finite Elements in Analysis and Design.* – 2002. – Vol 38. – P. 1115–1130.
8. **Kelly B., Costello B.** FEA modeling of setting and mechanical testing of aluminum blind rivets // *Journal of Materials Processing Technology.* – 2004. – Vol. 153. – P. 74–79.
9. **Kliger R., Al-Emrani M.** FE analysis of stringer-to-floor-beam connections in riveted railway bridges // *Journal of Constructional Steel Research.* – 2003. – Vol 59. – P. 803–818.
10. **Langrand B., Deletombe E., Markiewicz E. et al.** Numerical approach for assessment of dynamic strength for riveted joints // *Aerospace Science and Technology.* – 1999. – Vol. 3. – P. 431–466.
11. **Langrand B., Deletombe E., Markiewicz E. et al.** Riveted joints modeling for numerical analysis of airframe crashworthiness // *Finite Elements in Analysis and Design.* – 2001. – Vol 38. – P. 21–44.
12. **Langrand B., Patronelli L., Deletombe E. et al.** An alternative numerical approach for full-scale characterization for riveted joints // *Aerospace Science and Technology.* – 2002. – Vol. 6. – P. 343–354.
13. **Liao M., Shi G., Xiong Y.** Analytical methodology for predicting fatigue life distribution of fuselage splices // *International Journal of Fatigue.* – 2001. – Vol 23. – P. 177–185.
14. **Liu L., Sawa T.** Stress analysis and strength evaluation of single-lap adhesive joints combined with rivets under external bending moment // *Journal of Adhesion in Science and Technology.* – 2001. – Vol 15., No 1. – P. 43–61.
15. **Lucas F.M., Silva J.P., Goncalves F. et al.** Multiple-site damage in riveted lap joints: experimental simulation and finite element prediction // *International Journal of Fatigue.* – 2000. – Vol. 22. – P. 319–338.
16. MSC/Patran 2004- “User's manual- Modeling and analysis guidelines”.
17. **Neves L., Cruz P., Henriques A.** Reliability analysis of steel connection components based on FEM // *Engineering Failure Analysis.* – 2001. – Vol 8. – P. 29–48.
18. **Terada H.** Structural fatigue and joint degradation // *International Journal of Fatigue.* – 2001. – Vol 23. – P. 21–30.
19. **Urban M.R.** Analysis of the fatigue life of riveted sheet metal helicopter airframe joints // *International Journal of Fatigue.* – 2003. – Vol 25. – P. 1013–1026.
20. **Witek L.** Numerical analysis of the initial stress forming in the process of blind riveting // *Proceedings of 7-th International Conference TECHNOLOGIA 2001, Bratislava - Slovakia.* – 2001. – Vol 2. – P. 736–739.
21. **Witek L.** Numerical and experimental analysis of preliminary stress, limiting load and fatigue life of blind riveted joints // *Journal of Theoretical and Applied Mechanics.* – 2005. – Vol 42. – P. 309–325.
22. **Witek L.** Numerical-experimental analysis of stability and limiting load of cylindrical shell reinforced by stringers in the shape of closed formers subjected to torsion: Doctor's thesis. – Rzeszow: Rzeszow University of Technology, 2002 /in Polish/.
23. **Witek L., Kopecki T., Mazurek P.** The problem of load capacity and stress distribution of thin-walled sheet duralumin adhesive-riveted joints // *Proceedings of the 4-th International Scientific Colloquium CAX TECHNIQUES.* – Bielefeld.- Germany, 1999. – P. 73–78.
24. **Xiong Y.** Analytical and finite element modeling of riveted lap joints in aircraft structure // *AIAA Journal.* – 1999. – Vol 37.